Journal of Thermal Analysis and Calorimetry (2020) 142:461–471
https://doi.org/10.1007/s10973-020-09627-6

Human skin thermal properties determination using a calorimetric sensor

P. J. Rodríguez de Rivera[1,2] · Mi. Rodríguez de Rivera[1] · F. Socorro[1] · M. Rodríguez de Rivera[1] · G. M. Callicó[2]

Received: 29 August 2019 / Accepted: 23 March 2020 / Published online: 9 April 2020

Abstract
The purpose of the calorimetric sensor developed is to measure the heat flux transmitted by conduction between the human body surface and a thermostat located inside the sensor. The measurement surface has an area of 2×2 cm^2. We have verified that the measured heat flux decreases linearly with the increase in the thermostat temperature. This allows us to define an equivalent thermal resistance between the internal temperature of the human body and the temperature of the thermostat. This equivalent thermal resistance can be determined by measuring the heat flux for different constant temperatures of the thermostat. An alternative is to perform a single measurement with linear programming of the thermostat temperature. With this type of measurement and from the calorimetric signal, it is also possible to determine an equivalent heat capacity of the skin in the measurement zone. In this article, we present the modelling and simulation of the sensor operation when the thermostat temperature varies linearly. We also present experimental measurements performed on the human body and with reference Joule dissipations.

Keywords Direct calorimetry · Heat conduction calorimeters · Human skin · Medical calorimetry · Thermal resistance · Thermal capacity

Introduction

A specially designed calorimetric sensor has been developed to directly measure the heat flux dissipated by the surface of the human body when the sensor is placed on the skin. This heat flux is transmitted by conduction between the human skin and a thermostat located inside the sensor. Two prototypes have been developed, the first one with a detection surface of 6×6 cm^2 [1–4] and the second one with a detection surface of 2×2 cm^2 [5–8]. Both prototypes share the same principle of operation, although the second one, smaller in size, has smaller time constants and can be applied more easily to the skin. These sensors can be included in the group of non-differential heat conduction calorimeters [9].

In the normal operation of this sensor, the measurements are made with its thermostat at a constant temperature. However, making measurements for different constant temperatures of the thermostat (between 24 and 36 °C, below 37 °C) we verify that the measured power decreases when the thermostat temperature is increased. This experimental fact allows defining a total thermal resistance between the skin and the sensor thermostat. The thermal resistance of the sensor, measured experimentally, is lower than the total thermal resistance, which allows evaluating an equivalent thermal resistance of the 2×2cm^2 skin area [7, 8]. Based on these experimental results, a study of the operation of the sensor has been carried out for the case in which the temperature of the thermostat has a linear variation. This study begins with a modelling of the instrument that simulates the

✉ M. Rodríguez de Rivera
manuel.rguezderivera@ulpgc.com

P. J. Rodríguez de Rivera
pedrojrdrs@gmail.com

Mi. Rodríguez de Rivera
miriam.mrdrs@gmail.com

F. Socorro
fabiola.socorro@ulpgc.com

G. M. Callicó
gustavo@iuma.ulpgc.es

[1] Departamento de Física, Universidad de Las Palmas de Gran Canaria, 35017 Las Palmas de Gran Canaria, Spain

[2] Instituto Universitario de Microelectrónica Aplicada (IUMA), Universidad de Las Palmas de Gran Canaria, 35017 Las Palmas de Gran Canaria, Spain

operation of the sensor in this situation. The model parameters are obtained from experimental measurements corresponding to Joule dissipations. The modelling and simulation allow us proposing a method to correctly determine the power that passes through the sensor (which comes from the surface of the human body or the calibration base) and thereby determining the equivalent thermal resistance of the skin. In addition, these measurements with linear variation in the thermostat temperature allow determining the equivalent heat capacity of the skin in the measurement zone.

The medical applications of this sensor are still to be determined, but we can affirm that direct calorimetric measurements can complement the measurements of the surface temperature of the human body made with digital thermography. There are currently numerous studies based on digital thermography on the interaction between human thermophysiology and the external environment [10, 11]. In other cases, local temperatures can be used in the study of thermoregulation of the human body for different activities [12, 13] and to monitor and detect various pathologies [14–16].

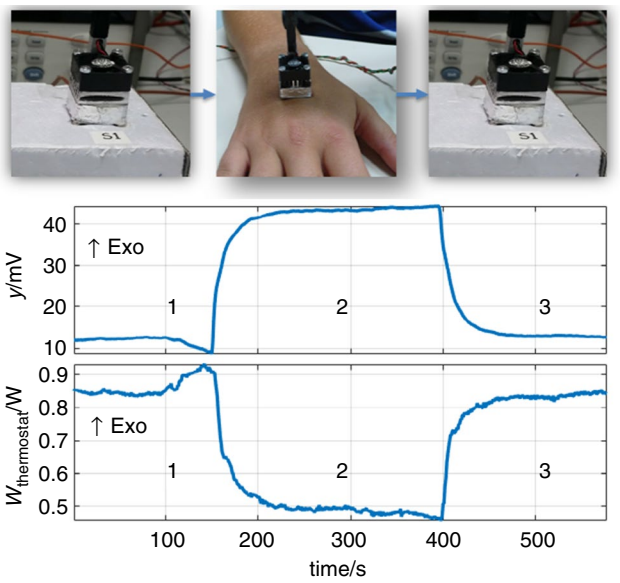

Fig. 1 Measurement method and example for a thermostat constant temperature of 28 °C; (1) and (3) sensor at its base; (2) sensor on human skin. Calorimetric signal (y) and thermostat power ($W_{\text{themostat}}$)

Experimental system

The experimental system has already been described in previous works [5–8]. The main element of the calorimetric sensor is a thermopile located between an aluminum plate and a thermostat that is at a programmed temperature. The measurement surface has an area of 2×2 cm^2. The purpose of the device is the determination of the heat flow that is transmitted by conduction between the surface of the human body and the thermostat. This heat flow crosses the thermopile of measurement, which is what provides the calorimetric signal. The calculation of heat flow (W_{body}) is performed using the ratio given by Eq. (1) (in Laplace domain).

$$Y(s) = \frac{K_1 \cdot (1 + s\tau_1^*)}{(1 + s\tau_1) \cdot (1 + s\tau_2)} \cdot W_{\text{body}}(s) + \frac{K_2 \cdot (1 + s\tau_2^*)}{(1 + s\tau_1) \cdot (1 + s\tau_2)} \cdot W_{\text{thermostat}}(s) \quad (1)$$

being Y the calorimetric signal, W_{body} the power dissipated by the human body and that passes through the sensor, and $W_{\text{thermostat}}$ the power dissipated in the thermostat. The parameters of the transfer functions (TFs) are determined by Joule calibrations. For this purpose, a base with an electrical resistance for sensor calibration is used. Table 1 indicates the parameters of these transfer functions.

Table 1 Parameters of the *TFs* of the calorimetric sensor (Eq. 1)

K_1/mVW^{-1}	K_2/mVW^{-1}	τ_1/s	τ_2/s	τ_1^*/s	τ_2^*/s
105.4	−54.86	121	12	92	146

The calibration base is used to position the sensor before and after each measurement made on the human body in order to have the initial and final baselines. A basic measurement in the human body for a programmed thermostat temperature has three phases: (1) the sensor is placed on the calibration base until the set temperature reaches the steady state (initial baseline); (2) the sensor is placed on the surface of the human body for the required time (1–5 min.); and finally, (3) the sensor is returned to the base until the signals return to their initial baseline. Figure 1 shows an example of the measurement procedure.

The measurement and control program is written in C++ and controls, through USB/GPIB interface, the data acquisition system and the programmable power supply. The sampling period of the measurements is 1 s. Currently, two sensors are available, allowing us to make cross-measurements. In previous studies, all these elements and the measurement and control instrumentation are described in detail [5–8].

Measures with the thermostat at constant temperature

This section shows an example of applying measurements on the skin of the human body with the constant temperature sensor thermostat. Figure 2 shows the case of four consecutive measurements made on the sternum area of

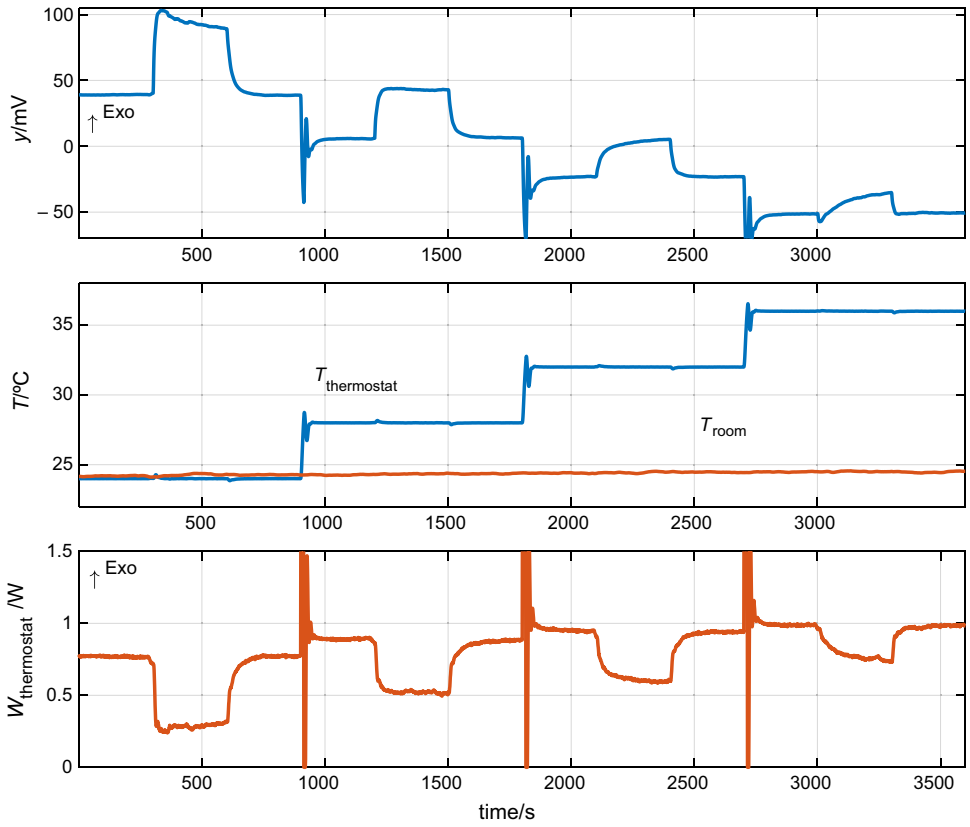

Fig. 2 Calorimetric signal (y), room and thermostat temperatures (T_{room}, $T_{thermostat}$) and dissipated power in the thermostat ($W_{thermostat}$) for the case of four consecutive measurements made on the sternum area of a healthy 60-year male subject (T_{room} = 24.4 °C, $T_{thermostat}$ = 24, 28, 32, 36 °C)

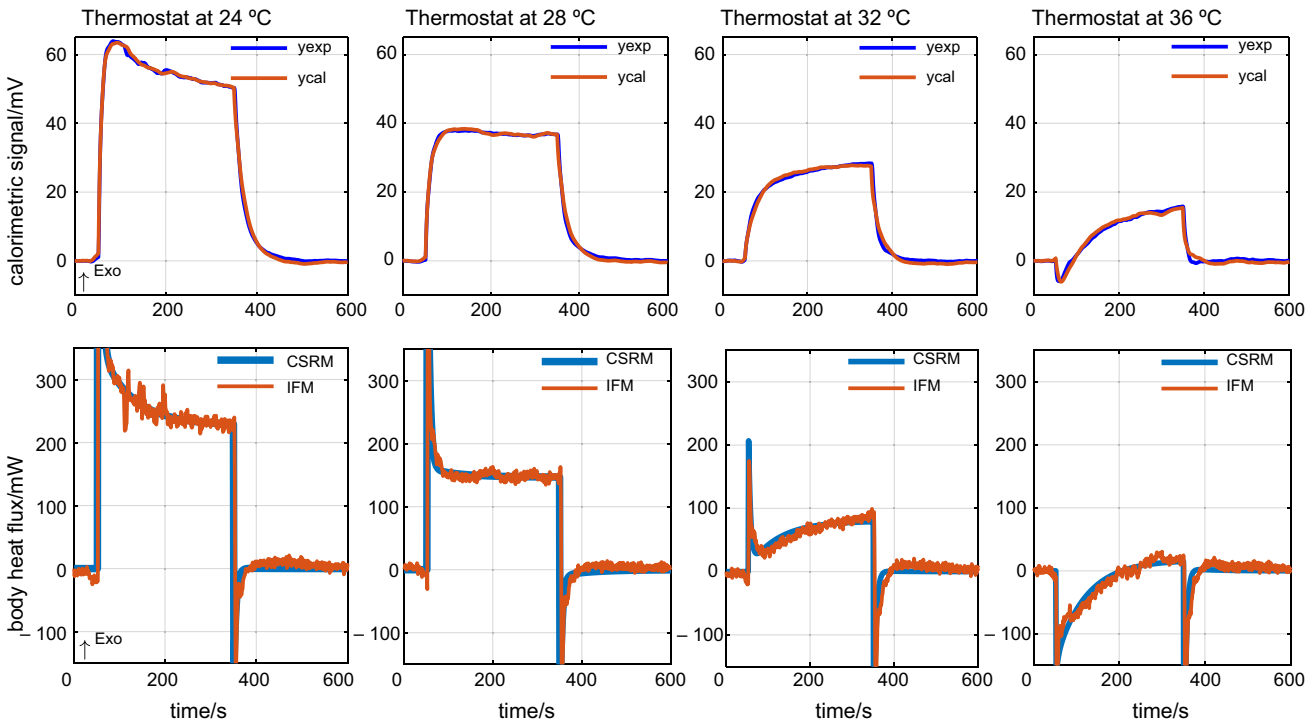

Fig. 3 Calorimetric signal and power calculated by CSRM and IFM for the case of measurements (Fig. 2) made on the sternum area of a healthy 60-year male subject in resting state, for thermostat temperatures of 24, 28, 32 and 36 °C (T_{room} = 24.4 °C)

a healthy 60-year male subject, in a resting state (seated) and dressed normally. The subject had not been exercising prior to the measurements. The room temperature was $T_{room} = 24.4 \pm 0.2$ °C. The RH was approximately 65%, and room airflow is avoided. These four measurements correspond to four temperatures of the sensor's thermostat: 24, 28, 32 and 36 °C. Figure 2 shows the calorimetric signal, the room and thermostat temperatures, and the power dissipated in the sensor's thermostat.

Figure 3 shows the calculation results of the power transmitted from the human body zone to the thermostat, made with two methods [8]: in blue, the power determined by the calorimetric signal reconstruction method (CSRM) and, superimposed in red, the power obtained by the inverse filtering method (IFM). Additionally, the figures represent the experimental calorimetric signal (in blue) and the calculated one (in red) by the CSRM. We can see a good approximation of the reconstructed signal, even in the cases of very low signal–noise ratio. In these cases, the CSRM allows obtaining the coefficients of the sum of exponentials that describes the temporal function of the power:

$$\begin{aligned} W(t) &= 0 && \text{for} \quad t < t_1 \\ W(t) &= A_0 + A_1 \exp(-t/\tau_1) + A_2 \exp(-t/\tau_2) && \text{for} \quad t_1 \le t < t_2 \\ W(t) &= A'_1 \exp(-t/\tau_1) + A'_2 \exp(-t/\tau_2) && \text{for} \quad t \ge t_2 \end{aligned} \tag{2}$$

being t_1 the instant the sensor is placed on the human body and t_2 the instant it is returned to its base. Among all the performed measurements, we study the most appropriate time constants for the calorimetric signal reconstruction, resulting: $\tau_1 = 5$ s and $\tau_2 = 70$ s, both for the time interval the sensor is placed on the human body and for the time interval it is returned to its base.

Table 2 shows the values obtained for coefficients A_0, A_1, A_2, A'_1 and A'_2 for each of the four measurements (Figs. 2 and 3). The coefficients A_1, A_2, A'_1 and A'_2 are the amplitudes of the terms of the power that represent the transient states corresponding to the placement of the sensor on the skin (A_1 and A_2) and the transient of the repositioning of the sensor on its base (A'_1 and A'_2). Parameter A_0 directly represents the power transmitted from the skin to the sensor thermostat for the steady state. It is easy to check the linear variation in parameters A_0, A_1, A_2 with the thermostat temperature. The inverse of the slope of this line has thermal resistance units (KW^{-1}).

Analysing the results, we observe that the inverse of the slope of A_0 represents the total thermal resistance (R_{total}) between the skin and the thermostat. Experimentally determined [5] the thermal resistance of the sensor ($R_{sensor} = 12$ KW^{-1}), the equivalent thermal resistance of the skin can be determined by the expression: $R_{skin} = R_{total} - R_{sensor} = 57.4 - 12 = 45.4$ KW^{-1}. It is interesting to realize that these values (57.4, 12.0 and 45.4) are very similar to the inverses of the slopes of A_0, A_1 and A_2. This is because A_1 represents the instantaneous heat flux (time constant of 5 s) as a consequence of the difference in temperatures between the sensor and skin surfaces, and the coefficient A_2 represents the equalization of the skin temperature (70 s time constant).

Measures with linear variation in the thermostat temperature

Model

An alternative to the experimental measurement described in the previous section is to program a linear variation in the thermostat temperature. It is thus possible to directly determine the heat flow transmitted from the skin to the sensor based on the thermostat temperature. This type of measurement will provide the thermal resistance and heat capacity of the skin in the measured area. In order to be able to relate the calorimetric signal with the variations in the power and with the heat capacity of the measurement zone, it is necessary to propose a model that adequately

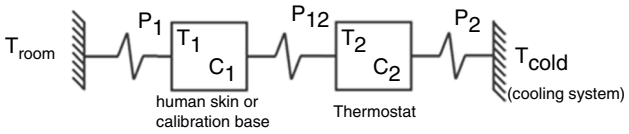

Fig. 4 Calorimetric sensor's model

Table 2 Values of parameter A_i of the power (Eq. 2) corresponding to the measurements in Figs. 2 and 3

Thermostat (T_{therm})	A_0/mW	A_1/mW	A_2/mW	A'_1/mW	A'_2/mW	Error/mW
24 °C	227.3	976.8	128.8	−163.1	0.8	±0.3
28 °C	146.8	457.7	14.1	−196.7	−9.5	±0.3
32 °C	80.0	200.1	−73.3	−305.9	1.2	±0.3
36 °C	17.2	−25.8	−155.2	−395.3	3.8	±0.3
Pearson's correlation coef. (A_i vs. T_{therm})	−0.998	−0.978	−0.997	−0.982	0.433	
Slope/mWK^{-1}	−17.4	−81.6	−23.5	−20.1	–	
Equivalent thermal resistance/KW^{-1}	57.4	12.2	42.6	49.6	–	

represents the operation of the sensor. For this purpose, we apply a modelling widely used in calorimeters by heat conduction [17–20].

For this calorimetric sensor, we propose a simple two-body model (Fig. 4) in which C_2 represents the heat capacity of the sensor thermostat and C_1 the heat capacity of the domain where the dissipation that passes through the sensor takes place and which is to be measured. If the sensor is at its base, C_1 represents the copper foil where the calibration resistance is located. However, when the sensor is applied to the skin of the human body, C_1 represents the surface area of the body that transmits the heat flow through the sensor. T_1 and T_2 are the temperatures of each domain. P_{12} is the thermal conductivity between the two domains; its inverse is the thermal resistance of the sensor. P_1 is the thermal conductivity of the first domain with the environment. P_2 is the thermal conductivity between the second domain and the cooling system.

The energy balance of each domain allows writing the system of equations Eq. (3) that relates the temperatures and powers developed in each domain.

$$\begin{aligned} W_1(t) &= C_1\frac{\mathrm{d}T_1}{\mathrm{d}t} + P_1\cdot(T_1 - T_{\mathrm{room}}) + P_{12}\cdot(T_1 - T_2) \\ W_2(t) &= C_2\frac{\mathrm{d}T_2}{\mathrm{d}t} + P_2\cdot(T_2 - T_{\mathrm{cold}}) + P_{12}\cdot(T_2 - T_1) \end{aligned} \tag{3}$$

During the measurement, the ambient temperatures and the cold focus (T_{room} and T_{cold}) are constant. In consequence, it is possible to correct the baselines of all variables (T_1, T_2, W_1 and W_2) and obtain an equivalent system of equations in which T_{room} and T_{cold} do not appear. Then curves T_1, T_2, W_1 and W_2 have zero value at the coordinate origin for time (Eq. 4).

$$\begin{aligned} W_1(t) &= C_1\frac{\mathrm{d}T_1}{\mathrm{d}t} + P_1T_1 + P_{12}\cdot(T_1 - T_2) \\ W_2(t) &= C_2\frac{\mathrm{d}T_2}{\mathrm{d}t} + P_2T_2 + P_{12}\cdot(T_2 - T_1) \end{aligned} \tag{4}$$

We assume that the calorimetric signal is a linear combination of the temperatures of the two bodies between which the thermopile of measurement is located, in the form: $y = k_1T_1 - k_2T_2$. Clearing T_1 and substituting in the first equation of the previous system (Eq. 4), we obtain a differential equation that relates the calorimetric signal $y(t)$, the temperature of the thermostat $T_2(t)$ and the power $W_1(t)$ developed in the C_1 domain:

$$W_1(t) = \frac{1}{k_{\mathrm{y}}}\left(\tau_{\mathrm{y}}\frac{\mathrm{d}y}{\mathrm{d}t} + y\right) + \frac{1}{k_{\mathrm{T}}}\left(\tau_{\mathrm{T}}\frac{\mathrm{d}T_2}{\mathrm{d}t} + T_2\right) \tag{5}$$

being:

$$\begin{aligned} \tau_{\mathrm{y}} &= \frac{C_1}{P_1 + P_{12}} \qquad \tau_{\mathrm{T}} = \frac{k_2\cdot C_1}{k_2\cdot P_1 + (k_2 - k_1)P_{12}} \\ k_{\mathrm{y}} &= \frac{k_1}{P_1 + P_{12}} \qquad k_{\mathrm{T}} = \frac{k_2}{k_2\cdot P_1 + (k_2 - k_1)P_{12}} \end{aligned} \tag{6}$$

When there is a linear programming of the thermostat temperature ($\mathrm{d}T_2/\mathrm{d}t$ = constant), in the human body there is also a linear variation in the heat flux between the skin surface and the thermostat ($\mathrm{d}W_1/\mathrm{d}t$ = constant). This is experimentally tested with different measurements on the surface of the skin for different constant temperatures of the thermostat, as described in the previous section. In this situation, Eq. (5) can be analytically solved and its solution is given by Eq. (7).

$$\begin{aligned} y &= y_0 + a_{\mathrm{y}}\cdot t + b_{\mathrm{y}}\cdot(1 - e^{-\mathrm{t}/\tau\mathrm{y}}) \quad \text{for} \quad t_1 \le t \le t_2 \\ y &= y_{\mathrm{f}} + b_{\mathrm{y}}\cdot(1 - e^{-\mathrm{t}/\tau\mathrm{y}}) \quad \text{for} \quad t \ge t_2 \end{aligned} \tag{7}$$

Linear temperature programming takes place from $t = t_1$ to $t = t_2$. For $t > t_2$, the thermostat temperature remains constant. The values y_0 and y_{f} are the values of the calorimetric signal for instants t_1 and t_2, respectively. The constants a_{y} and b_{y} are related to $\mathrm{d}W_1/\mathrm{d}t$ and with $\mathrm{d}T_2/\mathrm{d}t$ and are defined by the expressions of Eq. (8). They show the dependence of these parameters with the heating rate and other variables.

$$a_{\mathrm{y}} = k_{\mathrm{y}}\frac{\mathrm{d}W_1}{\mathrm{d}t} - \frac{k_{\mathrm{y}}}{k_{\mathrm{T}}}\frac{\mathrm{d}T_2}{\mathrm{d}t} \qquad b_{\mathrm{y}} = -\tau_{\mathrm{y}}k_{\mathrm{y}}\frac{\mathrm{d}W_1}{\mathrm{d}t} - \left(\tau_{\mathrm{y}} - \tau_{\mathrm{T}}\right)\frac{k_{\mathrm{y}}}{k_{\mathrm{T}}}\frac{\mathrm{d}T_2}{\mathrm{d}t} \tag{8}$$

For the measurement proposed in this work, initially the thermostat is kept at a constant temperature. When the steady state is reached, the sensor is placed in the area of the skin where the measure will take place, keeping the temperature constant. Once the steady state has been reached in the skin and keeping the sensor motionless, a linear variation in the thermostat temperature is programmed. Next, the thermostat temperature is kept constant again, and finally, the sensor is removed from the skin and placed in its base. This will be the operational method to be used in both simulations and experimental measurements.

Simulation

A constant thermostat temperature of +4 K above the ambient temperature is programmed in the simulation of the sensor operation. When the steady state is reached, a power $W_1 = 0.2$ W is dissipated in the base. Then, we decrease the power linearly ($-0.4\ \mathrm{mWs^{-1}}$) to a value of 0.1 W, and simultaneously, we increase the temperature of the thermostat linearly ($20\ \mathrm{mKs^{-1}}$) up to +9 K above the room temperature, keeping this temperature until the end of the measurement. At time $t = 1150$ s, the dissipation at the base ceases ($W_1 = 0$). This measure aims to simulate the sensor's

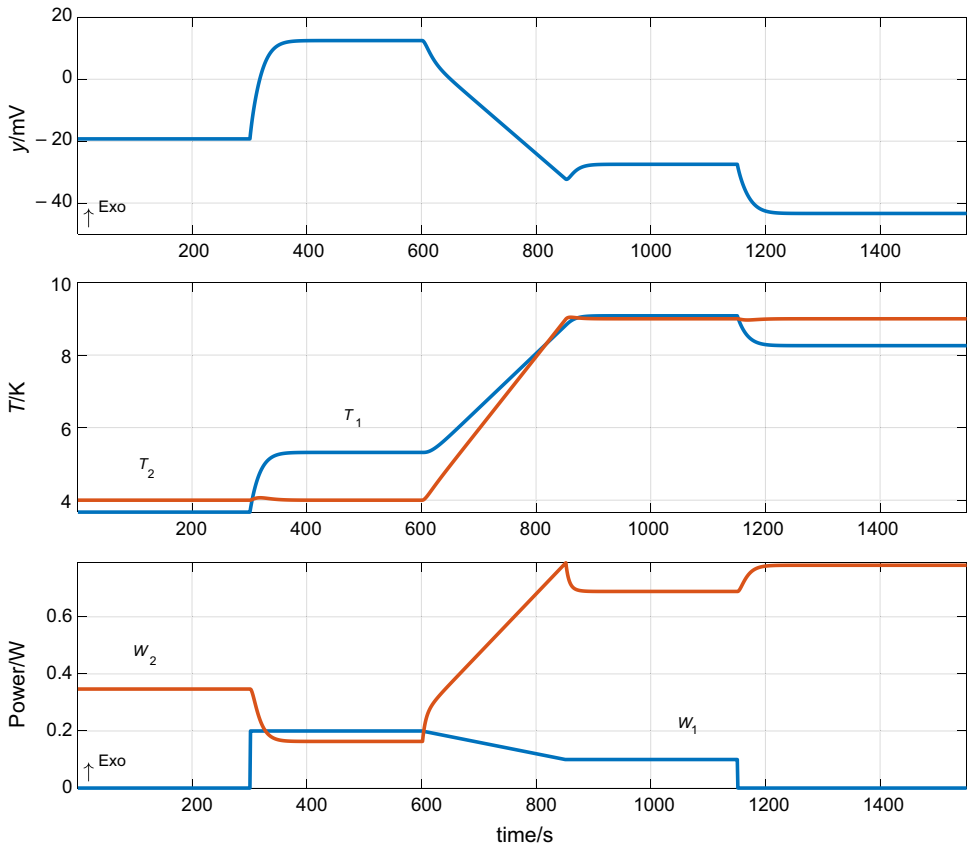

Fig. 5 Simulated measurement. Calorimetric signal (y), temperatures of the base (T_1) and thermostat (T_2), powers dissipated in the base (W_1) and in the thermostat (W_2)

Table 3 Parameters of the calorimetric sensor model (Fig. 4 and Eq. 4)

C_1/JK^{-1}	C_2/JK^{-1}	P_1/mWK^{-1}	P_2/mWK^{-1}	P_{12}/mWK^{-1}	k_1/mVK^{-1}	k_2/mVK^{-1}
2.0	3.656	10.0	77.57	111.53	19.3	22.53
Calorimetric signal: $y = k_1\, T_1 - k_2\, T_2$						

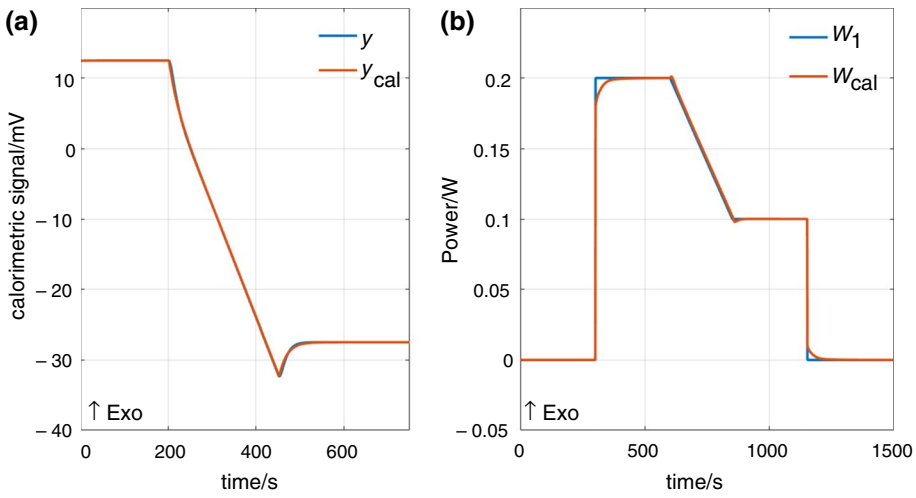

Fig. 6 Simulated measurement: **a** adjustment of the calorimetric signal with Eq. (7), **b** deconvolution of the signal using Eq. (1)

operating method when applied to the skin. Figure 5 shows the calorimetric signal, the temperatures of the base and the thermostat, and the dissipated powers in the base and in the thermostat.

In the simulation, the two-body model previously described is used and whose parameters have been determined by adjusting the simulated curves with experimental measurements. Table 3 shows the values of the model parameters.

Determination of heat capacity and heat flow

This section proposes a method for determining the heat capacity. For this purpose, the calorimetric signal in the ramp is studied: from $t=600$ s to $t=850$ s (Fig. 5), in such section the curve has the shape given by Eq. (7): $y(t)=y_0+a_y t+b_y[1-\exp(-t/\tau_y)]$. But for $t\geq 850$ s (after the ramp) the calorimetric signal has the form: $y(t)=y_f-b_y[1-\exp(-t/\tau_y)]$, where y_f is the value of the curve $y(t)$ at the end point of the ramp. In the adjustment process, the parameters $\tau_y=16.46$ s, $a_y=-0.159$ mVs^{-1}, $b_y=17.62$ mV are obtained. The average square error in the adjustment is 6 µV. The optimization method used is based on the one proposed by Nelder and Mead [21–23]. Figure 6a shows the final adjustment of the process of identification of parameters a_y, b_y and τ_y.

The first expression of Eq. (6) is used to determine the value of C_1, resulting in $C_1=16.45/8.23=2$ JK^{-1}, a value that coincides with that used in the model. With this result, the validity of the method for determining the heat capacity of the domain where dissipation occurs is assessed. In this case, the sensor is always located at its base, and the heat flow is determined directly using Eq. (1). The result is shown in Fig. 6b.

Experimental measurement in the calibration base

Before applying this method to the human body, several experimental tests are performed on the calibration base. As in the simulated case, the sensor thermostat is programmed at a constant temperature of 25 °C, when the steady state is reached, a constant power of 200 mW is dissipated for 550 s. Next, a linear variation in the thermostat temperature from 25 to 30 °C in 250 s is programmed. Simultaneously, the power dissipated in the resistance of the base is varied linearly from 200 to 100 mW at the same time (250 s). Keeping the temperature constant at 30 °C, the dissipation of 100 mW is maintained for 550 s, and then, the dissipation ceases, maintaining the thermostat temperature at the programmed final temperature (30 °C). Figure 7a shows the calorimetric signal. Figure 7b shows the powers dissipated in the base (W_1) and the dissipated in the thermostat (W_2). Figure 7c shows the variation in the thermostat temperature (5 K in 250 s).

To determine the heat capacity of the base, the calorimetric curve is adjusted with the functions given by Eq. (7). In this identification process, we determine the parameters $\tau_y=20.34$ s, $a_y=-0.1518$ mVs^{-1}, $b_y=6.372$ mV.

It is of interest to relate the time constant of the calorimetric signal (τ_y) with the heat capacity C_1 representing the domain where dissipation W_1 takes place. According to the first relationship of Eq. (6): $\tau_y=C_1/(P_{12}+P_1)$.

Since $P_1 \ll P_{12}, \tau_y \approx C_1/P_{12}=C_1 R_{sensor}$. The thermal resistance of the sensor is determined experimentally [5], and

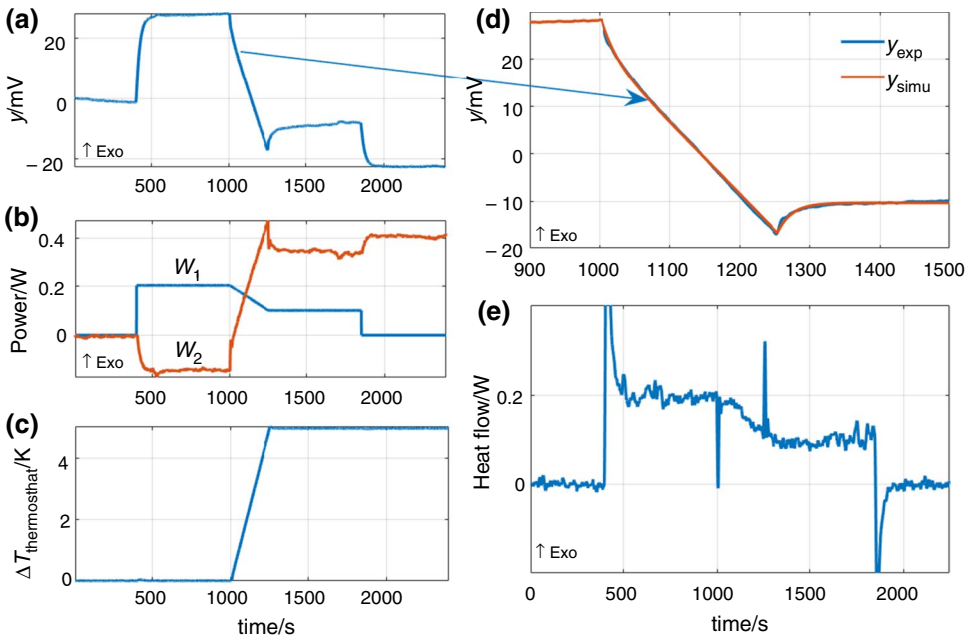

Fig. 7 Experimental measurement in the calibration base (all baselines have been adjusted): **a** calorimetric signal (y), **b** powers dissipated in the base (W_1) and in the thermostat (W_2), **c** thermostat temperature, **d** adjustment (Eq. 7) of zone of the calorimetric signal marked with an arrow, **e** heat flow (W_1 calculated with Eq. 1)

thus, we obtain the approximate relationship that relates the heat capacity to the time constant: $\tau_y \approx 12C_1$. In this measure, $C_1 = 20.34/12 = 1.695\ \mathrm{JK}^{-1}$.

Finally, we apply Eq. 1 to determine the power dissipated in the resistance located in the calibration base. The result (Fig. 7e) is adequate since the power values of 200 and 100 mW dissipated at the initial (25 °C) and final (30 °C) temperatures are correctly obtained. However, unwanted peaks appear in the deconvolution process before and after linear temperature variation. To avoid them, the method described in the next section is proposed.

Experimental measures in the human body

The measurement procedure on the surface of the human body is similar to those described in the previous sections and has the following phases:

(1) The sensor is placed in the base. A constant thermostat temperature of 28 °C is programmed.
(2) When the steady state is reached, the sensor (for 200 s) is applied to the skin in the indicated area, keeping the thermostat temperature constant (28 °C).
(3) Keeping the sensor on the skin, a linear variation in the thermostat temperature is programmed from 28 to 33 °C for 150 s.
(4) Next, without moving the skin sensor, and for 250 s, the thermostat temperature is maintained constant at 33 °C.
(5) Finally, the sensor is replaced in the base. The measurement requires a total of 600 s on the human body.

Table 4 Characteristics of the subjects (females)

	Age	Mass/kg	Height/m
Subject 1	23	54	1.55
Subject 2	20	74	1.68
Subject 3	20	88	1.68

Next, an experimental measurement is performed on the right thigh of a 20-year-old healthy female subject in a state of rest and horizontal position (subject 2 in Table 4). The room temperature was $T_{room} = 24.6$ °C. Figure 8 shows the calorimetric signal (Fig. 8a), the power dissipated in the thermostat (Fig. 8b) and the thermostat temperature (Fig. 8c).

To determine the heat flux dissipated by the surface of the human body, the following procedure is followed:

(1) Adjustment of the calorimetric signal corresponding to the linear temperature variation (from $t = 300$ s to $t = 450$ s) with the exponential function given by Eq. (7). Figure 8d shows three curves: the experimental curve (y_{exp}), the calculated curve (y_{simu1}) and the curve calculated by eliminating the exponential term (y_{simu2}). The parameters obtained are the following: $\tau_y = 66.9$ s; $a_y = -0.2249\ \mathrm{mVs}^{-1}$; $b_y = 27.0$ mV. The equivalent heat capacity of the skin in the measured area is $C_1 = \tau_y/R_{sensor} = \tau_y/12 = 5.575\ \mathrm{JK}^{-1}$. The mean square error of the adjustment is 48 μV ($N = 400$ points).
(2) Study of the area of the curve that represents the power of the thermostat when it varies linearly (from $t = 300$ s to $t = 450$ s). This area of the curve is adjusted with an exponential function similar to Eq. (7), and

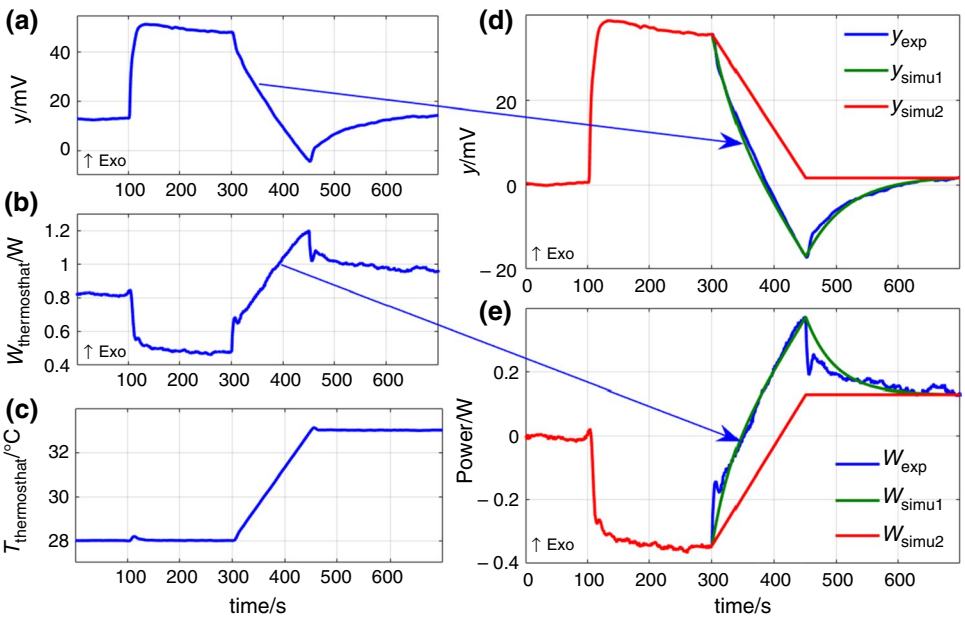

Fig. 8 Experimental measurement on the skin of the human body: **a** calorimetric signal (y), **b** power dissipated in the thermostat and **c** thermostat temperature. **d** Adjust (Eq. 7) of the zone of the calorimetric signal marked with an arrow. **e** Adjust (Eq. 7) of the zone of the power dissipated in the thermostat marked with an arrow

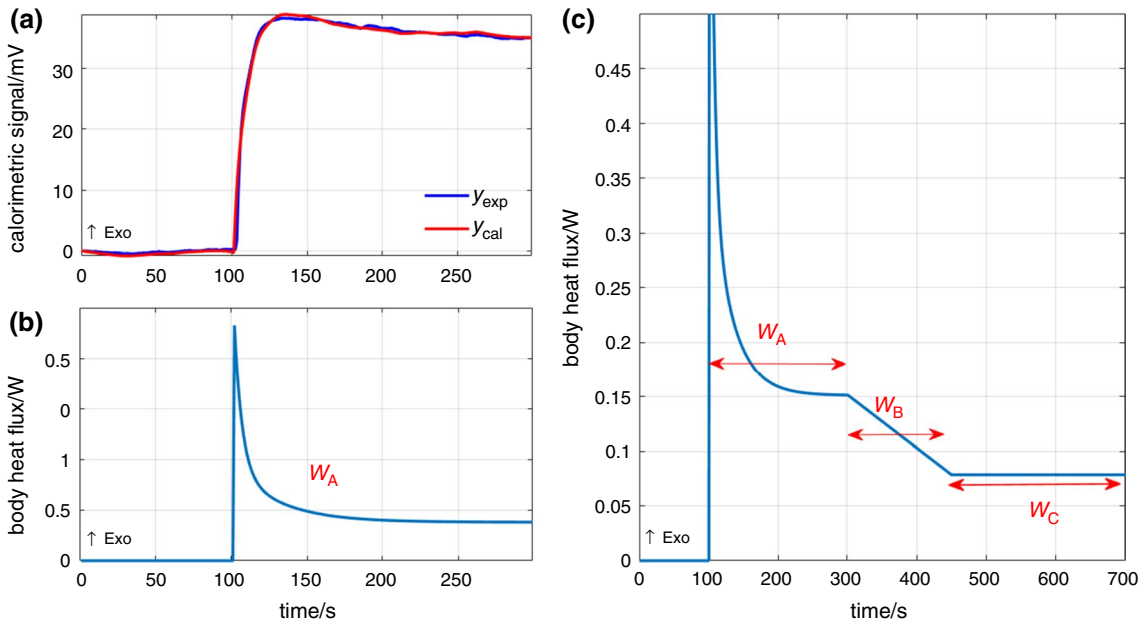

Fig. 9 Determination of heat flow dissipated by the surface of the human body. **a** Experimental calorimetric (y_{exp}) and calculated (y_{cal}) signals of the initial section. **b** Heat flow of the initial section (W_A). **c** Heat flux transmitted from the skin to the sensor as a function of time (W_A, W_B and W_C)

the following parameters are obtained: $\tau_W = 44.9$ s; $a_W = 3.1598$ mWs^{-1}; $b_W = -242.4$ mW. Figure 8e shows the experimental curve (W_{exp}), the calculated curve (W_{simu1}) and the curve calculated by eliminating the exponential term (W_{simu2}). The mean square error of the adjustment is 1.6 mW ($N = 400$ points).

(3) Study of the initial area of the measurement. By placing the sensor on the skin, the heat flow through the sensor can be represented as a sum of exponentials as indicated in Eq. (2). In this third phase, the heat flux is determined for this first measurement zone (from $t = 100$ s to $t = 300$ s) in which the thermostat is at a constant temperature of 28 °C. The calculation method has already been described in previous works [6, 7]. The exponential coefficients calculated are as follows: $A_0 = 150.9$ mW; $A_1 = 568.7$ mW; $A_2 = 210.3$ mW. The coefficient A_0 represents the steady state heat flux. The coefficient A_1 is the amplitude of the first exponential ($\tau_1 = 5$ s) that represents the initial peak of the power resulting from instantaneous contact between two surfaces that are at different temperatures (the surface of the sensor and that of the skin). A_2 is the amplitude of the second exponential (in this case $\tau_2 = 30.3$ s) and represents the transient prior to reaching the thermal equilibrium between the sensor and the skin. Figure 9a shows the experimental calorimetric curve (y_{exp}) and the calculated curve (y_{cal}). The mean square error of the adjustment is 43 µV ($N = 300$ points). The heat flux (W_A) dissipated by the skin and measured by the sensor is shown in Fig. 9b.

(4) Finally, the heat flow is determined as a function of three sections:

- Section A. From $t_1 = 100$ s to $t_2 = 300$ s. Constant thermostat temperature (28 °C).

$$W_A(t) = A_0 + A_1 \cdot e^{-(t-t_1)/\tau_1} + A_2 \cdot e^{-(t-t_1)/\tau_2}$$
$$A_0 = 150.9 \text{ mW};\ A_1 = 568.7 \text{ mW};\ A_2 = 210.3 \text{ mW} \quad (9)$$
$$\tau_1 = 5 \text{ s};\ \tau_2 = 30.3 \text{ s}$$

- Section B. From $t_2 = 300$ s to $t_3 = 450$ s. Linear variation in the thermostat temperature from 28 to 33 °C. In this section, the heat flux is determined

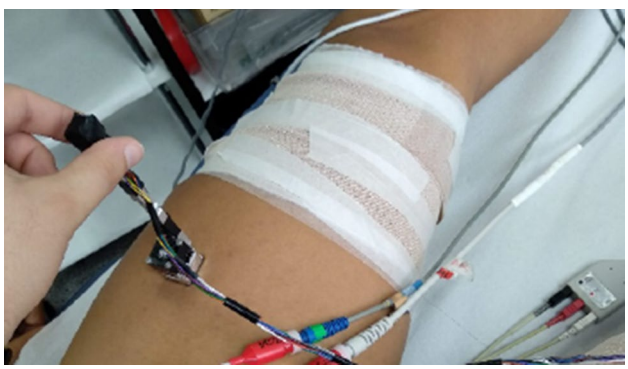

Fig. 10 Thigh sensor application

Table 5 Power in the initial section (W_A, $T_{thermostat} = 28$ °C) and in the final section (W_C, $T_{thermostat} = 33$ °C) of the measurement applied to three subjects (Table 4)

Subject	T_{room}/ °C	A_0/mW	A_1/mW	A_2/mW	τ_1/s	τ_2/s	W_C/mW	Error/mW
1	24.7	167.2	846.6	58.5	5	52.4	103.1	± 1.3
2	24.6	150.9	568.7	210.3	5	30.3	78.3	± 1.1
3	24.6	112.1	466.1	54.7	5	21.9	48.7	± 1.2
		$W_A(t) = A_0 + A_1\exp(-t/\tau_1) + A_2\exp(-t/\tau_2)$						

Table 6 Identification of the sections of the experimental curves corresponding to a linear variation in the temperature (Fig. 8)

Subject	Calorimetric signal (Fig. 8d)				Thermostat power (Fig. 8e)				Thermal properties		
	τ_y/s	a_y/mVs^{-1}	b_y/mV	ε_y/μV	τ_W/s	a_W/mWs^{-1}	b_W/mW	ε_w/mW	C_{skin}/JK^{-1}	R_{skin}/KW^{-1}	Error/KW^{-1}
1	64.7	−0.2243	21.2	45	35.4	3.2446	−249.4	1.6	5.39	63.9	± 1.5
2	66.9	−0.2249	27.0	48	44.9	3.1598	−242.4	1.6	5.58	56.1	± 1.2
3	69.9	−0.2135	23.2	42	38.5	3.0750	−249.9	1.6	5.83	66.4	± 1.5

Mean squared error of reconstructed signals are ε_y and ε_w. Equivalent heat capacity (C_{skin}) and thermal resistance (R_{skin}) are obtained in three subjects (Table 4)

with Eq. (1) for the steady state (the sensitivities of the transfer functions K_1 and K_2 are indicated in Table 1).

$$W_B(t) = W_A(t_2) + \frac{a_y \cdot (t - t_2) - a_W \cdot (t - t_2) \cdot K_2}{K_1}$$
$$a_y = -0.2249 \text{ mVs}^{-1};\ a_W = 3.1598 \text{ mW} \quad (10)$$

- Section C. From $t_3 = 450$ s to $t_4 = 700$ s. Constant thermostat temperature (33 °C).

$$W_C(t) = W_B(t_3) \quad (11)$$

The final result is shown in Fig. 9c. With this reconstruction of the power, the equivalent thermal resistance of the skin (R_{skin}) is determined, the temperature jump of the thermostat being $\Delta T = 5$ K, in a time interval $\Delta t = 150$ s. K_1 and K_2 are the sensitivities of the sensor *TFs* (Table 1).

$$R_{total} = \frac{\Delta T}{\Delta t} \cdot \frac{K_1}{a_y - a_W \cdot K_2} = 68.15 \text{ KW}^{-1}$$
$$R_{skin} = R_{total} - R_{sensor} = 68.15 - 12 = 56.15 \text{ KW}^{-1} \quad (12)$$

Note that 12 KW^{-1} is the thermal resistance of the experimentally obtained sensor [4].

Finally, the experimental results obtained in three different subjects are shown. The subjects are young women aged 20–23 years. All measurements were performed on the thigh, in the resting position and lying on a stretcher (Fig. 10). The mass and height of the subjects are indicated in Table 4. The average laboratory temperature was 24.7 °C.

The results in Table 5 correspond to the initial and final measurement zones, that is, for the constant temperatures of the thermostat of 28 °C (W_A) and 33 °C (W_C). The power dissipated when the sensor is applied to the skin is different for each subject.

Table 6 shows the results of the analysis of the measurement zone corresponding to the linear variation in the thermostat temperature for the three subjects studied. The parameters allow determining the equivalent heat capacity and thermal resistance of the measured area. The results obtained are different for each subject, but in terms of thermal resistance they are of the same order of magnitude as those obtained in a previous work [8]. This work shows the ability of the sensor to measure the heat flux and thermal properties of a superficial and localized area of the human body.

Conclusions

The validity of the sensor to measure the heat flux dissipated by the skin in a specific area of the human body for different thermostat temperatures has been assessed. A measurement with linear temperature variation can provide more information. To work in such conditions, it has been necessary to carry out a modelling and several simulations. This has allowed defining an appropriate measurement and calculation procedure.

Experimental measurements have been made in the human body and with Joule dissipations of reference. The experimental results show the ability of the sensor to determine an equivalent heat capacity and thermal resistance of the skin in the measurement zone. The equivalent thermal resistance values obtained are of the same order as those obtained in the previous work. The measurements with

linear variation in temperature shown in this work have been performed in three healthy subjects in a state of rest. This work is a preliminary study of the sensor's capacity for this mode of operation. It is necessary to perform a larger and deeper study with more subjects in different conditions. The human body's surface dissipation and its thermal properties are very variable. Therefore, it is necessary to develop techniques able to determine the thermal properties in a short period of time. The proposed method allows to determine the thermal properties of a skin area in a single measurement that takes 10 min, although we are working to reduce even more the measurement time. The medical applications of the sensor are yet to be determined. Currently, its greatest utility is the identification of thermal properties of the skin in a non-invasive way.

Acknowledgements The authors would like to acknowledge Professor J.A. López Calbet for his help in the experimental measurements performed in "Laboratorio de Rendimiento Humano de la Universidad de Las Palmas de Gran Canaria".

Funding This work was completed while Pedro Jesús Rodríguez de Rivera was beneficiary of a pre-doctoral grant given by the "Ministerio de Ciencia, Innovación y Universidades (Spain)" (No. FPU18/02990) and the "Agencia Canaria de Investigación, Innovación y Sociedad de la Información del Gobierno de Canarias (Spain)" (No. TESIS2019010023).

References

1. Socorro F. Rodríguez de Rivera M (2010) Development of a calorimetric sensor for medical application. Part I. Operating model. J Therm Anal Calorim. 2010;99:799–802.
2. Jesús Ch, Socorro F, Rodríguez de Rivera M. Development of a calorimetric sensor for medical application. Part II. Identification and simulation. J Therm Anal Calorim. 2013;113:1003–7.
3. Jesús Ch, Socorro F, Rodríguez de Rivera M. Development of a calorimetric sensor for medical application. Part III. Operating methods and applications. J Therm Anal Calorim. 2013;113:1009–13.
4. Jesús Ch, Socorro F, Rodríguez de Rivera HJ, Rodriguez de Rivera M. Development of a calorimetric sensor for medical application. Part IV. Deconvolution of the calorimetric signal. J Therm Anal Calorim. 2014;116:151–5.
5. Socorro F, Rodríguez de Rivera PJ, Rodríguez de Rivera M. Calorimetric minisensor for the localized measurement of surface heat dissipated from the human body. Sensors. 2016;16:1864.
6. Socorro F, Rodríguez de Rivera PJ, de Rivera Rodríguez, Mi Rodríguez, de Rivera M. Mathematical model for localised and surface heat flux of the human body obtained from measurements performed with a calorimetry minisensor. Sensors. 2017;17:2749.
7. Rodríguez de Rivera PJ, de Rivera Rodríguez, Mi Socorro F, Rodríguez de Rivera M. Method for transient heat flux determination in human body surface using a direct calorimetry sensor. Measurement. 2019;39:1–9.
8. Rodríguez de Rivera PJ, de Rivera Rodríguez, Mi Socorro F, Rodríguez de Rivera M. Measurement of human body surface heat flux using a calorimetric sensor. J Therm Biol. 2019;81:178–84.
9. Hansen LD. Toward a standard nomenclature for calorimetry. Thermochim Acta. 2001;371:19–22.
10. Lahiri BB, Bagavathiaappan S, Jayakumar T, Philip J. Medical applications of infrared thermography: a review. Infrared Phys Technol. 2012;55:221–35.
11. Livingston S, Nolan R, Frim J, Reed L, Limmer R. A thermographic study of the effect of body composition and ambient temperature on the accuracy of mean skin temperature calculations. Eur J Appl Physiol Occup Physiol. 1987;56:120–5.
12. Dębiec-Bąk A, Kuligowski T, Skrzek A. Analyzing thermoregulation processes in early school-age girls and boys through thermography. J Therm Anal Calorim. 2019. https://doi.org/10.1007/s10973-019-08843-z.
13. Kasprzyk T, Cholewka A, Kucewicz M, Sieron K, Sillero-Quintana M, Morawiec T, Stanek A. A quantitative thermal analysis of cyclists' thermo-active base layers. J Therm Anal Calorim. 2019;136:1689–99.
14. Godoy SE, Hayat MM, Ramirez DA, Myers SA, Padilla RS, Krishna S. Detection theory for accurate and non-invasive skin cancer diagnosis using dynamic thermal imaging. Biomed Opt Express. 2017;8(4):2301–23.
15. Nowak I, Mraz M, Mraz M. Thermography assessment of spastic lower limb in patients after cerebral stroke undergoing rehabilitation. J Therm Anal Calorim. 2019. https://doi.org/10.1007/s10973-019-08844-y.
16. Kasprzyk-Kucewicz T, Cholewka A, Bałamut K, Kownacki P, Kaszuba N, Kaszuba M, Stanek A, Sieroń K, Stransky J, Pasz A, Morawiec T. The applications of infrared thermography in surgical removal of retained teeth effects assessment. J Therm Anal Calorim. 2020. https://doi.org/10.1007/s10973-020-09457-6.
17. Isalgue A, Ortin J, Torra V, Viñals J. Heat flux calorimeters: dynamical model localized time constants. An Fis. 1980;76:192–6.
18. Socorro F, de Rivera MR, Jesús Ch. A thermal model of a flow calorimeter. J Therm Anal Calorim. 2001;64:357–66.
19. Socorro F, de la Nuez I, Rodríguez de Rivera M. Calibration of isothermal heat conduction calorimeters: case of flow calorimeters. Measurement. 2003;33:241–50.
20. Kirchner R, de Rivera MR, Seidel JM, Torra V. Identification of micro-scale calorimetric devices. Part VI. An approach by RC-representative model to improvements in TAM microcalorimeters. J Therm Anal Calorim. 2005;82:179–84.
21. Lagarias JC, Reeds JA, Wright MH, Wright PE. Convergence properties of the Nelder–Mead simplex method in low dimensions. SIAM J Opt. 1998;9(1):112–47.
22. Nelder JA, Mead C. A simplex method for function minimization. Comput J. 1965;7:308–13.
23. Optimization ToolboxTM User's Guide (2004) 5th printing; Revised for Version 3.0 (Release 14); The MathWorks, Inc.: Natic, MA, USA.